



Palladium-Induced Lateral Crystallization of Amorphous-Germanium Thin Film on Insulating Substrate

Ruilong Xie,^{a,b} Thanh Hoa Phung,^a Mingbin Yu,^b Sue Ann Oh,^c
Sudhiranjan Tripathy,^{c,*} and Chunxiang Zhu^{a,*z}

^aSilicon Nano Device Laboratory, Department of Electrical and Computer Engineering, National University of Singapore, Singapore 119260

^bInstitute of Microelectronics, A*STAR, Singapore 117685

^cInstitute of Materials Research and Engineering, A*STAR, Singapore 117602

In this article, metal (palladium, Pd)-induced lateral crystallization (MILC) of amorphous-germanium (α -Ge) films prepared by room-temperature sputtering on an insulating material (SiO_2) is observed and investigated using micro-Raman microscopy and transmission electron microscopy. The planar α -Ge thin films were annealed at 300, 350, and 400°C in a N_2 ambient. The MILC phenomenon is not observed for the samples annealed at 300°C for 2 h, while the MILC phenomenon is observed for α -Ge films annealed at 350 and 400°C for 2 h with a lateral growth rate of ~ 1.1 and $1.3 \mu\text{m/h}$, respectively. A poly-Ge film with a 400°C annealing temperature exhibits a smaller full width at half-maximum and a higher intensity of the sharp c-Ge peak than that annealed at 350°C, which can be the promising material candidate for Si-based three-dimensional integrated circuit applications. © 2009 The Electrochemical Society. [DOI: 10.1149/1.3126496] All rights reserved.

Manuscript submitted February 16, 2009; revised manuscript received April 6, 2009. Published April 30, 2009.

Microelectronics has primarily been a Si-based technology for many years. As silicon devices scale down to their fundamental limits, high mobility semiconductor materials have been considered as alternative channel materials to further enhance the performance for the future generation devices beyond 22 nm technology nodes. In addition to device performance, a large power dissipation and a time delay arising from interconnects also present serious challenges. One solution to tackle these problems is to use three-dimensional integrated circuits¹ (3D ICs). Germanium (Ge) possesses both a higher carrier mobility and a lower melting temperature than Si, making it a very promising candidate for 3D ICs. Ge is also an attractive material for Si-based optoelectronic devices. Ge (or poly-Ge) photodetectors have been demonstrated on a Si substrate successfully.^{2,3} Forming crystallized Ge on an insulator at low temperature also offers great opportunity to integrate photonic devices at the top level of the 3D ICs.

Several techniques have been reported to form crystallized Ge on insulator (GeOI), such as rapid melt growth,⁴ laser annealing,⁵ solid phase crystallization,⁶ and metal-induced crystallization⁷ or metal-induced lateral crystallization⁸⁻¹⁰ (MILC). To meet the requirements for 3D ICs, the growth temperature of GeOI must be low enough ($< 450^\circ\text{C}$) such that the interconnect layers are unaffected by the thermal budget. Among the different ways of forming GeOI, MILC stands out because of its unique features in terms of the low thermal budget process, the high crystal quality of the film, and the batch compatible process. To identify suitable metal candidates to induce the lateral crystallization of Ge films, one of the main important criteria is low crystallization temperature. It has been reported that metals that form germanides at the lowest temperature (Cu, Pd, and Ni) can also provide the most significant reduction in the crystallization temperature of α -Ge.¹¹ For Cu, although MILC of Si has been reported, no kind of lateral growth has been reported for Ge unless a stress-assisted Cu-induced crystallization technique is used.⁹ For Ni, lateral crystallization of pure Ge was not observed at annealing temperatures from 450 to 600°C,¹² while lateral crystallization of the chemical-vapor-deposited α -Ge film is recently reported with a lower annealing temperature at 360°C.¹⁰ For Pd, MILC of Si has been reported;¹³ however, there is no report on the MILC of α -Ge. In this study, Pd, as another possible promising metal candidate for inducing the low temperature lateral crystallization for α -Ge, is experimentally investigated. The α -Ge film is deposited using sputtering, which has even lower cost than the chemical vapor deposition process.

Experimental

The starting wafers were p-type Si(100). After SC1 (5 min) + 1 kW megasonic + diluted HF (1:200, 120 s) standard chemical cleaning, a SiO_2 layer of 200 nm was thermally grown in a furnace tube. After that, a 100 nm thick α -Ge film was deposited using radio frequency sputtering at room temperature. A thin oxide film was then deposited at low temperature ($\sim 300^\circ\text{C}$) using plasma-enhanced chemical vapor deposition to protect the Ge layer immediately. After that, the α -Ge film was patterned and dry etched to form islands on the insulating substrate. Some windows were then opened for the metal contact. A thin Pd layer of ~ 4 nm was then deposited using an electron-beam evaporator and patterned using a lift-off process to prevent any unwanted metal contamination. The thin metal layer was chosen to favor the α -Ge crystallization because the Pd_xGe_y compound formation and amorphous Ge crystallization are mutually competitive processes.¹⁴ The test structure, as shown in Fig. 1, was used to investigate the MILC process in Ge. The samples are isothermally annealed in a N_2 ambient at atmosphere pressure for 2 h at 300, 350, and 400°C, respectively. The MILC regions were then subsequently investigated by Raman spectroscopy, high resolution transmission electron microscopy (HR-TEM), and selective area electron diffraction (SAED).

Results and Discussion

Micro-Raman spectroscopy using a 514.5 nm Ar^+ laser has been employed to evaluate the crystalline quality of the Ge MILC regions. The thin protecting oxide layer on Ge was chemically removed before the Raman measurement. Figure 2 shows the Raman

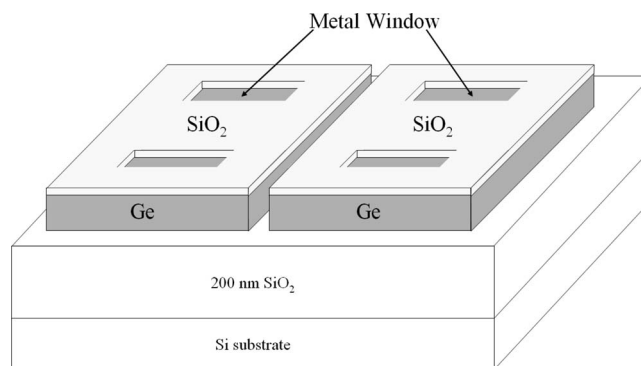


Figure 1. Structure used to investigate the lateral crystallization of the α -Ge thin film.

* Electrochemical Society Active Member.

^z E-mail: elezhucx@nus.edu.sg

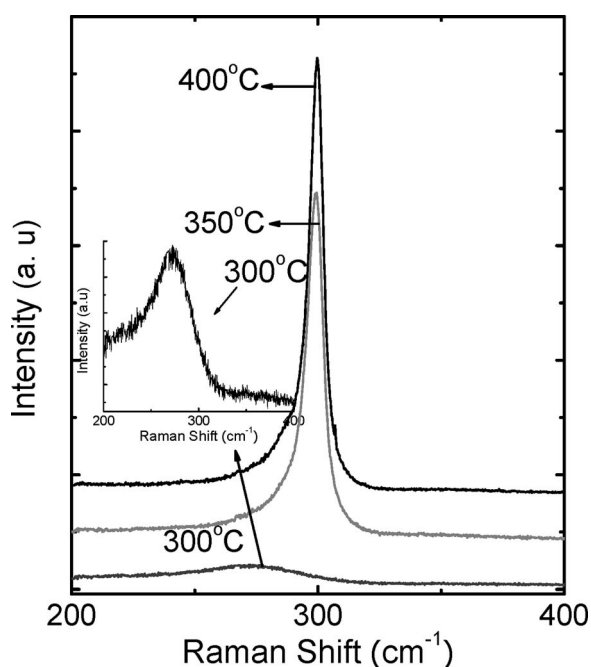


Figure 2. Raman spectra of the Ge lateral region obtained after 2 h annealing at 300, 350, and 400°C.

spectra for samples annealed at different temperatures. The sample annealed at 300°C has a broad peak centered at 272.5 cm^{-1} with a full width at half-maximum (fwhm) height of $\sim 54.6 \text{ cm}^{-1}$, as shown in the inset of Fig. 2. This peak is attributed to the scattering of local transverse optical phonons of amorphous Ge.¹⁵ Therefore, it can be seen that 300°C is not high enough for the MILC process to take place on the α -Ge film on the insulating material. When the annealing temperature is increased to 350°C, the Raman spectra of the Ge film at the MILC region is dominated by zone-center optical phonons in bulk c-Ge peaked at 299.6 cm^{-1} with a small asymmetric shoulder at lower frequencies. For the sample annealed at 400°C, the intensity of the main peak becomes even greater, suggesting the increase in Ge crystallinity in the film. Compared to bulk c-Ge phonon peaks at $\sim 301.4 \text{ cm}^{-1}$,¹⁶ a 1.8 cm^{-1} Raman shift to a lower frequency is observed for our MILC Ge films. This is possibly due to the tensile stress resulting from the lattice mismatch between germanide and crystalline Ge. It should also be noted that the volume shrinkage associated with the transformation of an amorphous

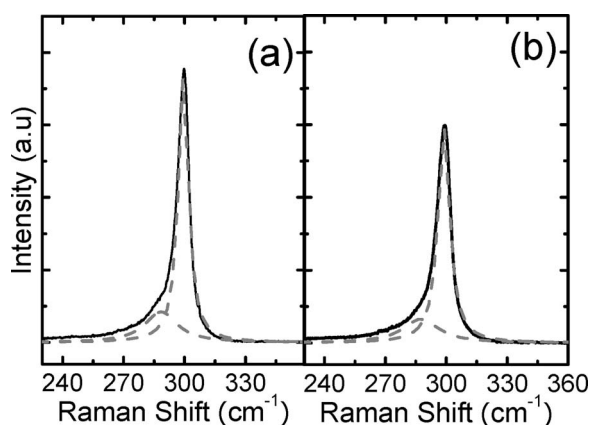


Figure 3. Raman spectra of the poly-Ge films deconvoluted into its components for (a) 400 and (b) 350°C annealed samples: Sharp peak at 299.6 cm^{-1} is due to the zone-center optical phonons in bulk c-Ge; the broader band peaking at $\sim 287.5 \text{ cm}^{-1}$ is due to Ge nanocrystals.

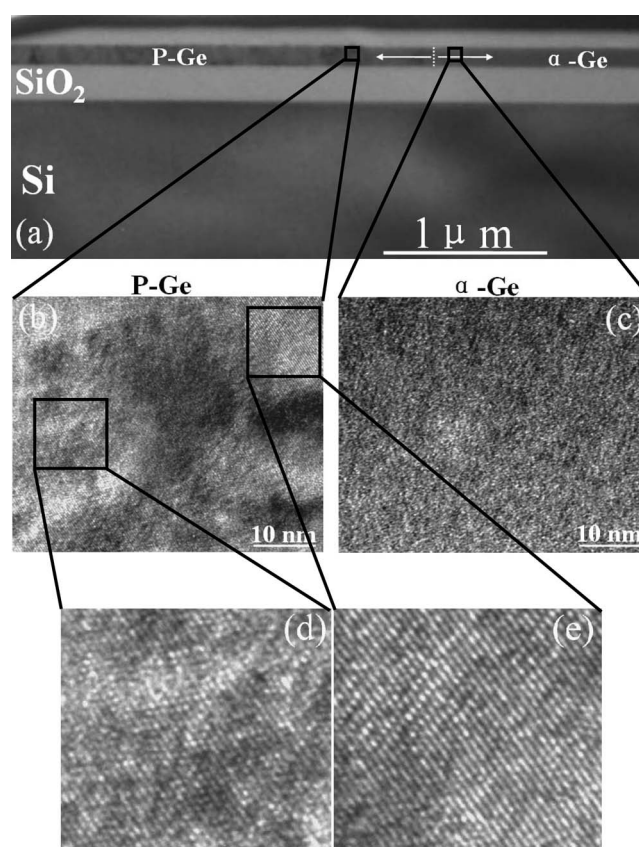


Figure 4. (a) XTEM image of a 100 nm thick α -Ge sample after annealing for 2 h at 400°C; (b) HRTEM image for the poly-Ge region; (c) HRTEM image for the α -Ge region; [(d) and (e)] magnified HRTEM image.

region into a denser, crystalline material will also cause the tensile stress. From the Raman peak shift for Ge, an in-plane strain ϵ_{\parallel} can be calculated from the relationship of strain vs phonon peak shift, $\Delta\omega = (1/\omega_0)[q - (C_{12}/C_{11})p]\epsilon_{\parallel} = B\epsilon_{\parallel}$,¹⁷ where C_{11} and C_{12} are elastic constants and q and p are phonon deformation potentials. Using the parameter in Ref. 18 for elastic constants and that in Ref. 19 for phonon deformation potentials, the proportionality factor $B = -415 \text{ cm}^{-1}$ with strain ϵ_{\parallel} of about 0.43% is obtained in the Ge film.

The Raman spectra for samples annealed at 400 and 350°C are further deconvoluted into its components, as shown in Fig. 3. The sharp peaks at $\sim 299.6 \text{ cm}^{-1}$ are due to the zone-center optical phonons in bulk c-Ge; the broader peaks at $\sim 287.5 \text{ cm}^{-1}$ are for Ge nanocrystals.²⁰ The amorphous Ge (peaked at $\sim 272 \text{ cm}^{-1}$) fraction is undetectable, suggesting that the MILC region is fully crystallized when the samples are annealed at 350°C or higher. The fwhm is 7.01 cm^{-1} for samples annealed at 350°C, and it decreases to 6.06 cm^{-1} when the annealing temperature increases to 400°C. This value is close to those of single-crystalline Ge (fwhm $\sim 4.5 \text{ cm}^{-1}$).²¹ The decrease in fwhm and the increase in intensity of the sharp c-Ge peak suggest that an increase in grain size and an increase in Ge crystallinity are obtained at higher annealing temperatures, which is confirmed by transmission electron microscopy (TEM). It should also be noted that a decrease in fwhm could also result from the defect reduction at higher annealing temperatures.

The MILC regions were further characterized using TEM. It was found that the minimum lateral growth lengths are ~ 2.2 and $2.6 \mu\text{m}$ for samples annealed at 350 and 400°C, respectively, which correspond to the MILC growth rates of $\sim 1.1 \mu\text{m/h}$ at 350°C and $1.3 \mu\text{m/h}$ at 400°C. Figure 4a shows the cross-sectional transmission electron microscopy (XTEM) picture for the MILC region and at the interface between poly-Ge and α -Ge after annealing at 400°C

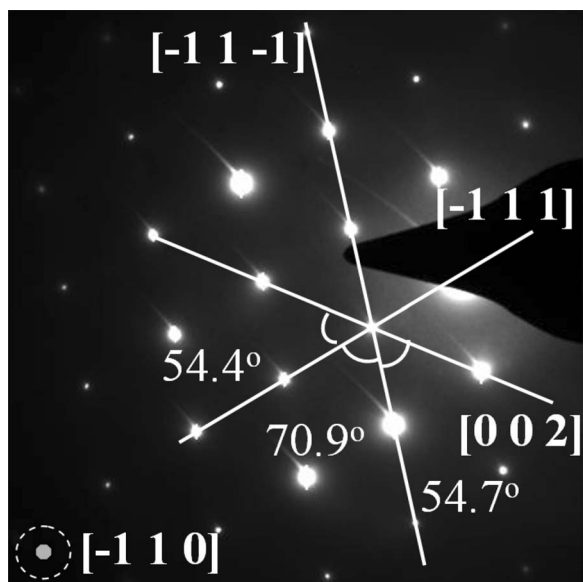


Figure 5. SAED pattern taken on the same area of Fig. 4b.

for 2 h. The HRTEM image and the magnified TEM images, as shown in Fig. 4b, d, and e, reveal that the MILC region is completely crystallized to very fine grains with sizes as large as ~ 100 nm. This is consistent with the Raman results. For comparison, Fig. 4c shows the HRTEM image for the α -Ge region; we can see that no crystallization takes place after 400°C annealing. Figure 5 shows the SAED pattern for the same region of Fig. 4b. The Ge orientations are $[\bar{1}\bar{1}\bar{1}]$, $[\bar{1}11]$, and $[002]$ when a beam axis of $[\bar{1}10]$ is assumed based on the angles in the SAED pattern.

It is clear that α -Ge crystallizes at much lower temperatures in metal/Ge thin films than that of an isolated α -Ge film. For Pd, the enhancement of crystallization at lower temperature is related to the thin germanide (Pd_2Ge) phase at the metal/ α -Ge interface, which is thought to act as a nucleus for Ge crystallization.¹⁴ Pd_2Ge has a hexagonal structure, and its basal plane (0001) is epitaxial on the (111) plane of Ge. Therefore, the crystallization of α -Ge may be initiated through epitaxial growth on previously crystallized Pd_2Ge at the $\text{Pd}_2\text{Ge}/\alpha$ -Ge interface. This crystallization can further simulate α -Ge crystallization in preferred sites, and finally the grain growth propagates into the lateral area if sufficient thermal energy is provided. According to Ref. 22 an interfacial reaction takes place when Pd is deposited on Ge at room temperature (forming Pd_2Ge). Larger 3D Pd_2Ge clusters are formed at 475 K, and the formation of faceted Pd_2Ge crystallites and a $(\sqrt{3} \times \sqrt{3})R30^\circ$ reconstruction on

the (0001) facets take place at 675 K.²³ This is why samples annealed at 400°C exhibit better MILC quality than samples annealed at 350°C .

Conclusions

Lateral crystallization of α -Ge planar films on an insulating material (SiO_2) induced by Pd has been observed and investigated using Raman microscopy and TEM. The MILC regions are fully crystallized with very fine grains. The lateral crystallization rates are ~ 1.1 and 1.3 $\mu\text{m}/\text{h}$ at 350 and 400°C , respectively. The high quality MILC poly-Ge thin film can be the promising material for Si-based 3D IC applications.

Acknowledgments

The authors acknowledge the helpful discussions with Yuwei Ma.

National University of Singapore assisted in meeting the publication costs of this article.

References

1. J.-H. Park, M. Tada, D. Kuzum, P. Kapur, H.-Y. Yu, H.-S. Philip Wong, and K. C. Saraswat, *Tech. Dig. - Int. Electron Devices Meet.*, **2008**, 389.
2. J. F. Liu, J. Michel, W. Giziewicz, D. Pan, K. Wada, D. D. Cannon, S. Jongthammanurak, D. T. Danielson, L. C. Kimerling, J. Chen, et al., *Appl. Phys. Lett.*, **87**, 103501 (2005).
3. G. Masini, L. Colace, and G. Assanto, *Opt. Mater. (Amsterdam, Neth.)*, **17**, 243 (2001).
4. Y. Liu, M. D. Deal, and J. D. Plummer, *Appl. Phys. Lett.*, **84**, 2563 (2004).
5. H. Watakabe, T. Sameshima, H. Kanno, T. Sadoh, and M. Miyao, *J. Appl. Phys.*, **95**, 6457 (2004).
6. I. Tsunoda, A. Kenjo, T. Sadoh, and M. Miyao, *Appl. Surf. Sci.*, **224**, 231 (2004).
7. F. Katsuki, K. Hanafusa, M. Yonemura, T. Koyama, and M. Doi, *J. Appl. Phys.*, **89**, 4643 (2001).
8. H. Kanno, K. Toko, T. Sadoh, and M. Miyao, *Appl. Phys. Lett.*, **89**, 182120 (2006).
9. B. Hekmatshoar, S. Mohajerzadeh, D. Shahrjerdi, and M. D. Robertson, *Appl. Phys. Lett.*, **85**, 1054 (2004).
10. J.-H. Park, P. Kapur, K. C. Saraswat, and H. Peng, *Appl. Phys. Lett.*, **91**, 143107 (2007).
11. S. Gaudet, C. Detavernier, A. J. Kellock, P. Desjardins, and C. Lavoie, *J. Vac. Sci. Technol. A*, **24**, 474 (2006).
12. H. Kanno, I. Tsunoda, A. Kenjo, T. Sadoh, and M. Miyao, *Appl. Phys. Lett.*, **82**, 2148 (2003).
13. Y.-S. Kim, M.-S. Kim, and S.-K. Joo, *J. Electrochem. Soc.*, **153**, H19 (2006).
14. Z. Chen, S. Zhang, S. Tan, and Z. Wu, *Mater. Sci. Eng., A*, **373**, 21 (2004).
15. Y. Sasaki and C. Horie, *Phys. Rev. B*, **47**, 3811 (1993).
16. T. H. Loh, H. S. Nguyen, C. H. Tung, A. D. Trigg, G. O. Lo, N. Balasubramanian, D. L. Kwong, and S. Tripathy, *Appl. Phys. Lett.*, **90**, 092108 (2007).
17. J. Zi, K. Zhang, and X. Xie, *Prog. Surf. Sci.*, **54**, 69 (1997).
18. *CRC Handbook of Chemistry and Physics*, CRC, Boca Raton (2003).
19. F. Cerdeira, C. J. Buchenauer, F. H. Pollak, and M. Cardona, *Phys. Rev. B*, **5**, 580 (1972).
20. G. Kartopu, A. V. Sapelkin, V. A. Karavanskii, U. Serincan, and R. Turan, *J. Appl. Phys.*, **103**, 113518 (2008).
21. S. Guha, M. Wall, and L. L. Chase, *Nucl. Instrum. Methods Phys. Res. B*, **147**, 367 (1999).
22. A. Hiraki, *J. Electrochem. Soc.*, **127**, 2662 (1980).
23. J. Wang, M. Li, and E. I. Altman, *J. Appl. Phys.*, **100**, 113501 (2006).